Grafting of poly(ethylene glycol) to poly-lysine augments its lifetime in blood circulation and accumulation in tumors without loss of the ability to associate with siRNA

Kano, Arihiro
Institute for Materials Chemistry and Engineering, Kyushu University

Moriyama, Kenji
Institute for Materials Chemistry and Engineering, Kyushu University

Yamano, Takeshi
Institute for Materials Chemistry and Engineering, Kyushu University

Nakamura, Izumi
Institute for Materials Chemistry and Engineering, Kyushu University

他

出版情報：Journal of Controlled Release. 149 (1), pp.2-7, 2011-01-05. Elsevier
バージョン：

Grafting of poly(ethylene glycol) to poly-lysine augments its lifetime in blood circulation and accumulation in tumors without loss of the ability to associate with siRNA

Arihiro Kano[1], Kenji Moriyama[1], Takeshi Yamano[1], Izumi Nakamura[1], Naohiko Shimada[1], and Atsushi Maruyama[1,2,*]

[1]Institute for Materials Chemistry and Engineering, Kyushu University, 744 Motooka, Nishi-ku, Fukuoka 812-8581, Japan
[1,2]CREST, Japan Science and Technology Agency, 4-1-8, Honcho, Kawaguchi, Saitama 332-0012, Japan

*Corresponding author. Institute for Materials Chemistry and Engineering, Kyushu University, 744 Motooka, Nishi-ku, Fukuoka 819-0395, Japan. Phone: +81 92 642 3097; Fax: +81 92 642 4224; E-mail address: maruyama@ms.ifoc.kyushu-u.ac.jp

Abstract

Poly-lysine has been studied as a carrier for the delivery of drugs and nucleic acids for at least a decade. It is an especially attractive carrier for DNA and RNA, because of its condensed cationic charges. In our previous study, we showed that poly(ethylene glycol) (PEG) grafted to poly-L-lysine (PLL) remarkably increased the life time of a small interfering RNA (siRNA) in blood circulation. In this study, we prepared a new series of PEG-grafted PLL (PLL-*g*-PEG) with various lengh (PEG 2 k, 5 k, 10 k Da and PLL 28 k and 40 k Da), to evaluate masking effects of PEG on cationic charges of PLL *in vivo* and the structural implications for biodistribution and tumoral accumulation. The best in the series, 40K10P37 (40 kDa of PLL, 10 kDa of PEG, 37 mol% grafting) with molecular weight of 10^6 as determined by Multi-Angle Laser Light Scattering (MALLS), accumulated in tumors at about 8% of the injected dose per gram of tissue. Interestingly, a PLL-*g*-PEG conjugate pre-mixed with murine sera prevented degradation of siRNA, suggesting that PLL-*g*-PEG preferentially associates with siRNA in sera. Our results indicate grafting of PEG to the side chains of PLL augments its lifetime in blood

circulation and tumoral accumulation without loss of the ability to associate with siRNA and support further evaluation of these cationic delivery carriers.

1. Introduction

Delivery carriers for therapeutic agents, including genes, oligonucleotides, and small molecule drugs, that insure drug stability and enhance biodistribution have the potential to revolutionize disease treatments. A large number of studies have been performed using liposomes, micelles, gels, polymers, and virus-mediated techniques (reviewed in [1-8]). Liposomes and micelles are self-assembled and size-controllable nanoparticles often used to encapsulate polar or lipophilic drugs, however, these self-assembled materials are often not stable enough in blood circulation. Hydrophilic polymeric materials normally determine the size of the complex depending on its own molecular mass with payloads. These above delivery carriers have been investigated for passive targeting to solid tumors. This targeting is based on the concept that soluble macromolecules, including serum proteins such as albumin or IgG, preferentially accumulate in solid tumors; this has been termed the enhanced permeability and retention (EPR) effect [9] (reviewed in [10]). N-(2-hydroxypropyl)methacrylamide (HPMA), a synthetic macromolecule, exhibits water solubility, low cytotoxicity, and low antigenicity. To date, HPMA has been reported as a delivery carrier for a variety of drugs, hormones, and genes (reviewed in [11]), however, it is not biodegradable nor metabolized *in vivo*.

Poly-lysine is a biocompatible material with condensed cationic charges that make it well suited to associate with anionic DNA or RNA. However, poly-lysine causes adverse effects on cells due to nonspecific random interactions attributed to the cationic charges. To prevent non-specific interactions, conjugation to hydrophilic or amphiphilic macromolecules, such as dextran or poly(ethylene glycol) (PEG), has been widely investigated (reviewed in [12]). Bogdanov et al. first reported use of PEG-grafted to PLL as a regent for magnetic resonance angiography [13]. MPEG-succcinate (5 kDa) was grafted to PLL (25 kDa) through amide bonds and the rest of the amino groups were substituted with diethyrenetriaminepentaacidic acid (DTPA) for gadolinium chelation. The authors reported no permanent immune response and observed accumulation in the

reticuloendothelial system. The same group also reported PEG-grafted PLL as a drug delivery carrier. In this case, the residual amine groups were succinylated and formed adducts with cis-diamminedichloroplatinum(II) (cisplatin) [14]. Choi et al. grafted 550 Da PEG to 25 kDa PLL through amide bonds at grafting ratio from 5 to 25 mol% [15] for a gene carrier and showed higher transfection efficiencies and lower cytotoxicities in the sample with 10 mol% grafting ratio. It is now widely recognized that PEG has a superior performance for stealth effects on many molecules including proteins *in vivo*, however, the fate of systemically injected PEG-grafted PLL remains to be elucidated.

We previously demonstrated PEG-grafted PLL (PLL-*g*-PEG) forms a complex with small interfering RNA (siRNA), prevents siRNA degradation *in vitro*, and extends the retention time in blood circulation compared to uncomplexed siRNA [16]. In this study, the lifetime in blood circulation and the biodistribution of PLL-*g*-PEG, including accumulation in tumors, was examined. We examined the effect of varying the length of PLL and PEG and the grafting ratio. In particular, PEG-grafted PLL has been investigated by amide bonding so far that dose not exhibit proper cationic charges on PLL. We utilized PEG-aldehyde to prepare PLL-*g*-PEG conjugates through the reductive amination reaction, based on the idea that the PEG-grafted secondary amine should be ionized under physiological condition.

2. Materials and methods

2.1. Materials

Poly-(L-lysine) hydrobromides (PLL) were purchased from Sigma-Aldrich Japan (Tokyo, Japan). Aldehyde-modified PEGs were gifted from NOF Corporation (Tokyo, Japan).

2.2. Preparation of PEG-grafted PLL

PLL-*g*-PEG was prepared as described previously [17-19]. Briefly, aldehyde-modified PEG was covalently coupled with the ε-amino groups of PLL by a reductive animation reaction in sodium borate buffer (pH 8.5) using sodium cyanoborohydride as a reductant.

The prepared PLL-*g*-PEG was purified by ultrafiltration, dialyzed against water, and then lyophilized. The PEG-grafting ratio was calculated from the results of elementary analysis (CHN-corder MT-6, Yanako, Kyoto, Japan) and verified by ^{1}H-NMR analysis (JNM-EX-270, JEOL, Tokyo, Japan). Molecular weights of the conjugates were evaluated by size-exclusion chromatography (model 800, JASCO, Japan) equipped with a multi-angle light scattering detector (DAWN HELEOS, Wyatt Technology, Santa Barbara, CA, USA). For some experiments, PLL-*g*-PEG was labeled with Alexa Fluor®647 succinimidyl ester (Invitrogen, Carlsbad, CA, USA) according to the manufacturer's instruction. The labeling ratios were adjusted to between 1 and 2 per PLL-*g*-PEG. The fluorescent intensity was measured and the normalized intensity was used for comparative experiments.

2.3. Animal work

All of the animal experiments were carried out under the guidance of the Animal Care and Use Committee, Kyushu, University.

2.3.1 Preparation of tumor-bearing mice

Mammary tumor 4T1 cells or colon tumor CT26wt cells were co-transfected with plasmid DNA, pGL3-control (Promega, Madison, WI, USA) and pPur (Clontech, Mountain View, CA, USA), by Lipofectamine 2000 (Invitrogen, Carlsbad, CA, USA), according to the manufacturer's instructions. Two days later, the transfected cells were transferred to a 96-well culture plate and grown in the presence of 10 μg/ml puromycin. Two weeks later, single colonies were selected under a microscope and subjected to the luciferase assay using Luciferase Assay System (Promega), according to the manufacturer's instructions. Luciferase-positive clones were selected and expanded for further experiments. Seven-week-old Balb/c mice were purchased from Kyudo Co., Ltd. (Tosu, Japan). Balb/c mice were injected with 3×10^5 tumor cells subcutaneously on the back. The tumors were allowed to grow until the diameters reached about 10 mm.

2.3.2. Biodistribution and tumor accumulation of PLL-*g*-PEG

The tumor-bearing mice were intravenously injected with 50 μg (based on PLL) of Alexa Fluor®647-labeled PLL-*g*-PEG. The fluorescence was observed and quantified using the IVIS® Lumina Imaging System (Xenogen Co., Alameda, CA, USA) at the indicated time; and average radiance is given. The metastatic lung tumor model was prepared by tail vain injection of 3 x 10^5 luciferase-expressing 4T1 tumor cells. The development of tumors in the lung was monitored by the luminescence imaging with the IVIS® Lumina Imaging System after intraperitoneal injection of 200 μl of 15 mg/ml luciferin (LUX Biotechnology, Edinburgh, United Kingdom). To determine biodistribution, liver, spleen, and tumor were removed 24 h after the injection and lysed with homogenizing buffer (20 mM Tris-HCl, pH 7.4, 150 mM NaCl, 1% Nonidet P-40 (NP-40), 0.1% SDS, 2 mM EDTA). The fluorescence of the homogenate was directly measured using a Wallac ARVO SX 1420 Multilabel Counter (Perkin Elmer, Waltham, MA, USA) using an excitation wavelength of 620 nm with emission monitored at 670 nm. The homogenate from a PBS-injected mouse was used as a control. The determined fluorescence intensity is presented as the percent of the injected dose per gram tissue.

2.3.3. Clearance of PLL-*g*-PEG from blood circulation

Alexa Fluor®647-labeled PLL-*g*-PEG was intravenously injected at 50 μg (based on PLL) per mouse. Blood was collected from orbital sinus at the indicated times. Blood samples (30 μl) were diluted to 100 μl with PBS and fluorescence was measured using Wallac ARVO SX 1420 Multilabel Counter. Percent of injected dose was calculated from the fluorescent intensity. The total blood volume was estimated from the following equation: Total blood volume (ml) = body weight (g) x 0.08 (ml/g)

2.4. siRNA stability in sera

Alexa® Fluor546-labeled siRNA was mixed with 90% of murine serum that included PLL-*g*-PEG (post-mixed) or were mixed with PLL-*g*-PEG and then added to 90% murine serum (pre-mixed). Transfection reagent JetPEI (Polyplus-transfection Inc. New York, NY, USA) was used as a control. The charge ratio of siRNA/PLL-*g*-PEG (NH_3^+/PO_4^-: N/P) was four. The siRNA was sequentially sampled after the mixing with serum and extracted by phenol/chloroform and ethanol precipitated. The extracted siRNA was

analyzed by 15% PAGE in TBE buffer. Agarose gel electrophoresis in TAE buffer was performed on the mixture of siRNA with PLL-*g*-PEG in PBS (137 mM NaCl, 2.7 mM KCl, 4.3 mM Na2HPO4, 1.4 mM KH2PO4, pH 7.4) or murine serum (post-mixed) after the incubation for 3 h, to verify the formation of the complex. The fluorescent was observed using LAS-3000 imaging system (FUJIFILM, Tokyo, Japan) after immersing of the gel in 1% SDS solution for 10 min. As a control, siRNA not mixed with PLL-*g*-PEG, was separated by a gel immediately after the mixing with serum.

3. Results

3.1 Preparation of a series of PLL-*g*-PEG conjugates

Since our previous results showed that higher molecular weight PLL and PEG conjugates extended the lifetime of siRNA in blood circulation better than lower molecular weight polymers, we used 28 kDa and 40 kDa PLL and 2 kDa, 5 kDa, and 10 kDa PEG to prepare PLL-*g*-PEG (Table I). To examine the effect of the length of the PEG side chain, the PEG-grafting ratio was carefully adjusted to about 36 mol%, except for 40K5P5. Conjugates were evaluated by elementary analysis and further verified by NMR analysis. The structure of PLL-*g*-PEG is shown in Figure 1. Our naming scheme indicates the PLL *M*w, the PEG *M*w, and the grafting ratio: For example, 28K5P36 indicates 28,000 *M*w PLL, 5,000 *M*w PEG, and 36 mol% grafting ratio. The prepared PLL-*g*-PEG was labeled with Alexa Fluor®647, in which labeling ratio was indicated in Table I.

3.2 Tumor accumulation of PLL-*g*-PEG

We first examined whether the prepared PLL-*g*-PEG accumulates in tumors. Alexa Fluor®647-labeled PLL-*g*-PEGs (50 μg based on PLL) were administrated via tail vein injection to 4T1 tumor-bearing mice and the fluorescence was observed using an IVIS® Lumina Imaging System (Fig. 2A). PLL-*g*-PEGs accumulated in tumors in a time-dependent manner, but the clearance rate was slower for 40K5P37 than for the other 28K5P36 (Fig.2A). The fluorescence images were further analyzed and quantitative

results are shown in Fig. 2B. All of the PLL-*g*-PEG accumulated in tumors; however, the accumulation of 28K5P36, 40K2P37, and 40K5P5 was not sustained. In contrast, 40K5P37 and 40K10P37 remained in tumors 100 h after injection, although these conjugates accumulated more slowly than the lower *M*w PLL-*g*-PEGs. Similar results were obtained in CT26 tumor-bearing mice (data not shown).

3.3 Biodistribution of PLL-*g*-PEG

To quantify the accumulated PLL-*g*-PEG, the tumor tissues were harvested at 24 h after the intravenous injection of Alexa Fluor®647-labeled PLL-*g*-PEG. The fluorescent intensities in the homogenized tumors were measured and percentage of injected dose per gram of tissue was calculated (Fig. 3A). Of the conjugates tested, 40K10P37 accumulated to the greatest extent; at 24 h after the injection, it was present in tumor at about 8% of the injected dose per gram tissue. The 28K5P36, 40K2P37, and 40K5P37 accumulated to between 3 and 5%; differences were not significant. *In vivo* fluorescence data indicated that PLL-*g*-PEG would mainly accumulate in liver and spleen. Accumulation in these organs was measured and is presented in Fig. 3B. 28K5P36 and 40K2P37 accumulated in liver to 11% and 20% of the injected dose per gram tissue, respectively, whereas about 50% of the injected dose of 40K5P37 and 40K10P37 per gram of tissue was found in liver. In spleen, accumulation was in order of 28K5P36 < 40K2P37 < 40K5P37 < 40K10P37.

3.4 Lifetime in blood circulation

Since it is thought that the tumor accumulation of macromolecules is correlated with stability in blood circulation, we examined the lifetime of PLL-*g*-PEG in mice. After tail vein injection of Alexa Fluor®647-labeled PLL-*g*-PEG, blood was collected and fluorescence was directly measured (Fig. 4). More than 70% of the injected dose of 40K10P37 remained in blood at 10 minutes after the injection and the other PLL-*g*-PEGs were detected at less than 30%. The clearance rate of the early stage correlated with the total molecular weight of the PLL-*g*-PEG, although less than 10% of the injected dose of all of PLL-*g*-PEGs remained in blood at 24 h after the injection,

3.5. Accumulation in metastatic lung tumors

To examine whether PLL-*g*-PEG accumulated in metastatic tumors, we administrated luciferase-expressing 4T1 tumor cells intravenously to a group of mice. The development of tumor cells in the lung was monitored based on luciferase activity using the IVIS® Lumina Imaging System. Alexa Fluor®647-labeled 40K5P37 was intravenously injected after tumor developed. The mice were euthanized 24 h after the injection of 40K5P37 and fluorescent images were obtained of the lungs (Fig. 5). The quantified fluorescent intensity was correlated with the level of the luminescence indicating the degree of the tumor development. Although background fluorescence was relatively high, it would be reduced if the time of visualization is optimized since the maximum accumulation of 40K5P37 and 40K10P37 in tumors was observed at 48 h or later after the injection as shown in Fig. 2B.

3.6 PLL-*g*-PEG stabilizes siRNA in sera

We previously demonstrated that the pre-injected PLL-*g*-PEG in murine tail vein effectively stabilized subsequently injected siRNA [16]. Here we examined whether 40K5P37 pre-mixed with murine sera could protect siRNA *in vitro*. 40K5P37 was first mixed with 90% of murine serum and Alexa Fluor546®-labeled siRNA was added 20 min later (post-mixed). The concentrations of 40K5P37 and siRNA were equivalent to those used in our *in vivo* analysis [16]. The phenol/chloroform-extracted siRNA was separated by PAGE and compared to siRNA pre-mixed with 40K5P37 and to siRNA pre-mixed with Jet PEI (Fig. 6A). The post-mixed siRNA was strikingly stable compared to that pre-mixed with Jet PEI, although the siRNA pre-mixed with 40K5P37 was the most stable. This result is consistent with our *in vivo* observations [16].

To demonstrate association of PLL-*g*-PEG with siRNA, the Alexa Fluor546®-labeled siRNA mixed with 40K5P37 in PBS was directly separated on an agarose gel. Free siRNA in PBS migrated toward the anode quickly (Fig. 6B, Alexa546 lane 1), while the siRNA mixed with 40K5P37 migrated slightly toward the cathode (Fig. 6B, Alexa546,

lanes 2, 3). The siRNA was observed with the 40K5P37 that was labeled with Alexa Fluor®647 (Fig. 6B, Alexa647, lane 3). These results indicate that 40K5P37 interacts with siRNA and migrates to a cathode with it. A Zimm plot analysis showed that the average molecular weights of 28K5P36 with or without 21-bp DNA, substituting for siRNA, were 5.6×10^5 and 4.3×10^5 and those of 40K5P37 were 8.1×10^5 and 6.4×10^5, respectively (Table II), suggesting that PLL-*g*-PEG did not aggregate; rather, it appears that the DNA/PLL-*g*-PEG complex consists of a single copolymer molecule and a single DNA duplex. Similar results were obtained when murine serum was used instead of PBS. Almost all of the siRNA mixed with 40K5P37 in serum migrated to the cathode (Fig. 6B, Alexa546, lane 6); however, the labeling of 40K5P37 with Alexa Fluor®647 interfered with interaction with siRNA as shown by the slightly reduced amount of siRNA that migrated toward the cathode (Fig. 6B, Alexa546, lane 7). When siRNA was mixed with murine serum without 40K5P37 and separated by an agarose gel immediately after the mixing, it migrated toward the anode. In serum, the migration was slower than that in PBS and even a much slower faint band was observed (Fig. 6B, Alexa546, lane 5, a and b, respectively). This may be the result of the interaction of siRNA with serum proteins. Together, these results indicate that 40K5P37 interacts with siRNA in sera and prevent degradation of the siRNA.

4. Discussion

We prepared a series of PEG-grafted PLLs using different length of PLLs (*M*w = 28 000 and 40 000) and PEGs (*M*w = 2 000, 5 000, and 10 000) with comparable grafting ratios to evaluate the effect of PEG side chains on the masking of cationic charges and accumulation of PLL in tumors *in vivo*. All of the prepared PLL-*g*-PEGs accumulated in tumors in mice, 28K5P36, 40K2P37, and 40K5P5 did not remain in the tumor, whereas 40K5P37 and 40K10P37 accumulated more slowly and remained in tumors at least 100 h. Interestingly, although the times of peak accumulation were different, the maximum accumulated amounts of 28K5P36 and 40K5P37 were similar. The total molecular mass may, at least in part, determine the maximum accumulation level. The property of the tumor accumulation was obviously reflected in the stability in blood circulation. More than 70% of the injected dose of 40K10P37 remained in blood at 10 minutes, whereas the

other PLL-*g*-PEG were detected at less than 30% of the injected dose after 10 minutes. However, all of the PLL-*g*-PEGs were reduced to less than 10% of the injected dose in blood at 24 h after the injection and a large fraction of 40K5P37 and 40K10P37 was found in liver and spleen. The lower molecular weight PLL-*g*-PEGs might be trapped by lung tissues in the first cycle of blood circulation. Our data indicates that the larger PLL, *M*w = 40,000, persists longest in tumors and the longer PEG, *M*w = 10,000, was particularly effective in keeping the level in blood circulation high immediately after injection. We used a 37 mol% of PEG grafting ratio; higher grafting may prevent entrapment by liver or spleen and should be investigated. Herein we also demonstrated PLL-*g*-PEG (40K5P37) accumulates in experimental lung metastatic tumors, depending on the size of the tumor. Interestingly, when 40K5P37 was added to serum and then siRNA was added, the PLL-*g*-PEG interacted with the siRNA, as shown by direct agarose gel electrophoresis, and protected the siRNA from degradation. In other words, PLL-*g*-PEG has a selective affinity to siRNA in serum. In this report, we showed that abundant and condensed cationic charges can be masked by controlling PEG-grafting. These results should facilitate the application of PLL-*g*-PEG conjugates in gene- and drug-delivery and tumor imaging.

Acknowledgements

We would like to gratefully acknowledge the Grant-in-Aid for Scientific Research (No. 16200034 and 20500410) from the Japan Society for the Promotion of Science (JSPS), the Joint Project for Materials Chemistry, and the 21st Century COE Program, “Functional Innovation of Molecular Informatics” from the Ministry of Education, Culture, Science, Sports and Technology of Japan for support of this research.

References

[1] M.L. Immordino, F. Dosio, L. Cattel, Stealth liposomes: review of the basic science, rationale, and clinical applications, existing and potential. Int J Nanomedicine 1(3) (2006) 297-315.

[2] I. Shapira, D.R. Budman, T. Bradley, R. Gralla, Evolving lipid-based delivery systems in the management of neoplastic disease. Oncology Reviews 3(2) (2009) 113-124.

[3] Y. Bae, K. Kataoka, Intelligent polymeric micelles from functional poly(ethylene glycol)-poly(amino acid) block copolymers. Advanced Drug Delivery Reviews 61(10) (2009) 768-784.

[4] S. Doktorovova, E.B. Souto, Nanostructured lipid carrier-based hydrogel formulations for drug delivery: a comprehensive review. Expert Opin Drug Deliv 6(2) (2009) 165-176.

[5] R. Singh, J.W. Lillard Jr, Nanoparticle-based targeted drug delivery. Experimental and Molecular Pathology 86(3) (2009) 215-223.

[6] S. Daya, K.I. Berns, Gene therapy using adeno-associated virus vectors. Clinical Microbiology Reviews 21(4) (2008) 583-593.

[7] U. Griesenbach, M. Inoue, M. Hasegawa, E.W.F.W. Alton, Sendai virus for gene therapy and vaccination. Current Opinion in Molecular Therapeutics 7(4) (2005) 346-352.

[8] L. Barzon, A.L. Stefani, M. Pacenti, G. Pal$\sqrt{\ }\pi$, Versatility of gene therapy vectors through viruses. Expert Opinion on Biological Therapy 5(5) (2005) 639-662.

[9] Y. Matsumura, H. Maeda, A new concept for macromolecular therapeutics in cancer chemotherapy: mechanism of tumoritropic accumulation of proteins and the antitumor agent smancs. Cancer Res 46(12 Pt 1) (1986) 6387-6392.

[10] H. Maeda, G.Y. Bharate, J. Daruwalla, Polymeric drugs for efficient tumor-targeted drug delivery based on EPR-effect. Eur J Pharm Biopharm 71(3) (2009) 409-419.

[11] J. Kopecek, P. Kopeckova, T. Minko, Z. Lu, HPMA copolymer-anticancer drug conjugates: design, activity, and mechanism of action. Eur J Pharm Biopharm 50(1) (2000) 61-81.

[12] M. Morille, C. Passirani, A. Vonarbourg, A. Clavreul, J.P. Benoit, Progress in developing cationic vectors for non-viral systemic gene therapy against cancer. Biomaterials 29(24-25) (2008) 3477-3496.

[13] A.A. Bogdanov, Jr., R. Weissleder, H.W. Frank, A.V. Bogdanova, N. Nossif, B.K. Schaffer, E. Tsai, M.I. Papisov, T.J. Brady, A new macromolecule as a contrast agent for MR angiography: preparation, properties, and animal studies. Radiology 187(3)

(1993) 701-706.

[14] A.A. Bogdanov, Jr., C. Martin, A.V. Bogdanova, T.J. Brady, R. Weissleder, An adduct of cis-diamminedichloroplatinum(II) and poly(ethylene glycol)poly(L-lysine)-succinate: synthesis and cytotoxic properties. Bioconjug Chem 7(1) (1996) 144-149.

[15] Y.H. Choi, F. Liu, J.S. Kim, Y.K. Choi, J.S. Park, S.W. Kim, Polyethylene glycol-grafted poly-L-lysine as polymeric gene carrier. J Control Release 54(1) (1998) 39-48.

[16] A. Sato, S.W. Choi, M. Hirai, A. Yamayoshi, R. Moriyama, T. Yamano, M. Takagi, A. Kano, A. Shimamoto, A. Maruyama, Polymer brush-stabilized polyplex for a siRNA carrier with long circulatory half-life. J Control Release 122(3) (2007) 209-216.

[17] A. Maruyama, M. Katoh, T. Ishihara, T. Akaike, Comb-type polycations effectively stabilize DNA triplex. Bioconjug Chem 8(1) (1997) 3-6.

[18] A. Maruyama, H. Watanabe, A. Ferdous, M. Katoh, T. Ishihara, T. Akaike, Characterization of interpolyelectrolyte complexes between double-stranded DNA and polylysine comb-type copolymers having hydrophilic side chains. Bioconjug Chem 9(2) (1998) 292-299.

[19] S.W. Choi, A. Yamayoshi, M. Hirai, T. Yamano, M. Takagi, A. Sato, A. Kano, A. Shimamoto, A. Maruyama, Preparation of cationic comb-type copolymers having high density of PEG graft chains for gene carriers. Macromolecular Symposia 249-250 (2007) 312-316.

Figure 1. Chemical structure of PLL-*g*-PEG

Figure 2. Accumulation of PLL-*g*-PEGs in tumors. A) Alaxa Fluor®647-labeled 28K5P36 and 40K5P37 were intravenously injected into 4T1 tumor-bearing mice. The fluorescence was observed at the indicated time. B) Time-dependent accumulation of PLL-*g*-PEGs in tumors. Alexa Fluor®647-labeled 28K5P36 (filled triangle), 40K2P37 (filled square), 40K5P5 (opened triangle), 40K5P37 (opened circle), and 40K10P37 (filled circle) were injected into 4T1 tumor-bearing mice. The fluorescence of the tumor sites was quantified by IVIS Lumina at the indicated time. Three mice were used for each conjugate.

Figure 3. Biodistribution of PLL-*g*-PEG in tumor-bearing mice. A) Alexa Fluor®647-labeled PLL-*g*-PEG was quantified 24 h after the injection and percent injected dose/g tissue in tumors is shown, B) Percent injected dose/g tissue in liver and spleen. Three mice were used for each conjugate.

Figure 4. Clearance of PLL-*g*-PEGs from blood circulation. Blood was collected from orbital sinus at the indicated times after the intravenous injection of Alexa Fluor®647-labeled PLL-*g*-PEGs and the fluorescence was measured as described in Material and methods. The values are percent of injected dose. Three mice were used for each conjugate.

Figure 5. Accumulation of PLL-*g*-PEG in metastatic tumors. Alexa Fluor®647-labeled 40K5P37 was intravenously injected into mice bearing metastatic lung model tumors. The lung was removed 24 h after the injection and developed in the luciferase buffer (100 mM Tris-HCl, pH 8.0, 10 mM MgSO4, 300 μM luciferin, 10 mM ATP, and 1 mg/ml BSA) for 1 min and the luminescence and fluorescence were observed. The quantified fluorescence intensity is represented under the photo.

Figure 6. The stability of siRNA post-mixed with PLL-*g*-PEG in murine serum. A) Alexa Fluor®546-labeled siRNA was pre-mixed or post-mixed with 40K5P37 in serum and extracted at the indicated time. The extracted siRNA was analyzed by PAGE. The siRNA pre-mixed with Jet PEI were similarly analyzed for comparison. B) Alexa

Fluor546-labeled siRNA was mixed with 40K5P37 (labeled with or without Alexa Fluor®647) in PBS or murine serum (post-mixed). After the 3 h, the mixture was analyzed by agarose gel electrophoresis and visualized by fluorescence. The siRNA alone was immediately analyzed to avoid degradation.

Table I. Preparation and characterization of PLL-*g*-PEG

Name	PLL	PEG	Molecular Weight			PEG Content		Fluorescent-labeing Ratio (fr)
	*M*w	*M*w	*M*w[a]/10[3]	*Mn*[a]*/10*[3]	*M*w[a]/*M*n[a]	(mole%)[b]	(wt%)[b]	dye/mol.
28K5P36(93)	28,000	5,000	420	167	2.5	36	93	1.7
40K2P37(84)	40,000	2,000	130	87	1.5	37	84	1.1
40K5P5(67)	40,000	5,000	83	53	1.6	5	67	1.7
40K5P37(94)	40,000	5,000	640	365	1.7	37	94	1.8
40K10P37(97)	40,000	10,000	1000	691	1.5	37	97	1.5

[a]Mn= the number-average molecular weight; Mw= the weight-average molecular weight. Mn and Mw were determined by MALLS. [b]Determined by ^{1}H NMR.

Table II. Weight average molecular weight and radius of gyration obtained by Zimm plot

DNA	*M*w/10[5]		RMS/nm	
	-	+ *	-	+ *
28K5P36(93)	4.3	5.6	29.4	24.1
40K5P37(94)	6.4	8.1	27.1	25

* 21-mer double staranded DNA was mixed at N/P = 2

Figure 1.

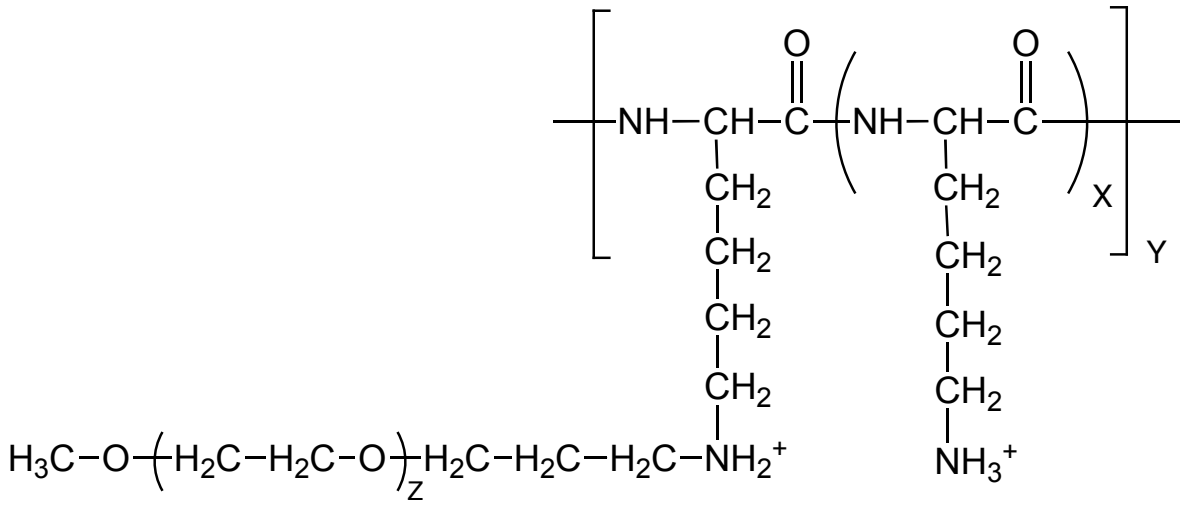
O
O
NH
CH
C
NH
CH
C
CH2
CH2
X
Y
CH2
CH2
CH2
CH2
CH2
CH2
CH2
H3C
O
H2C
H2C
O
Z
H2C
H2C
H2C
NH2+
NH3+

Figure 2.

A.

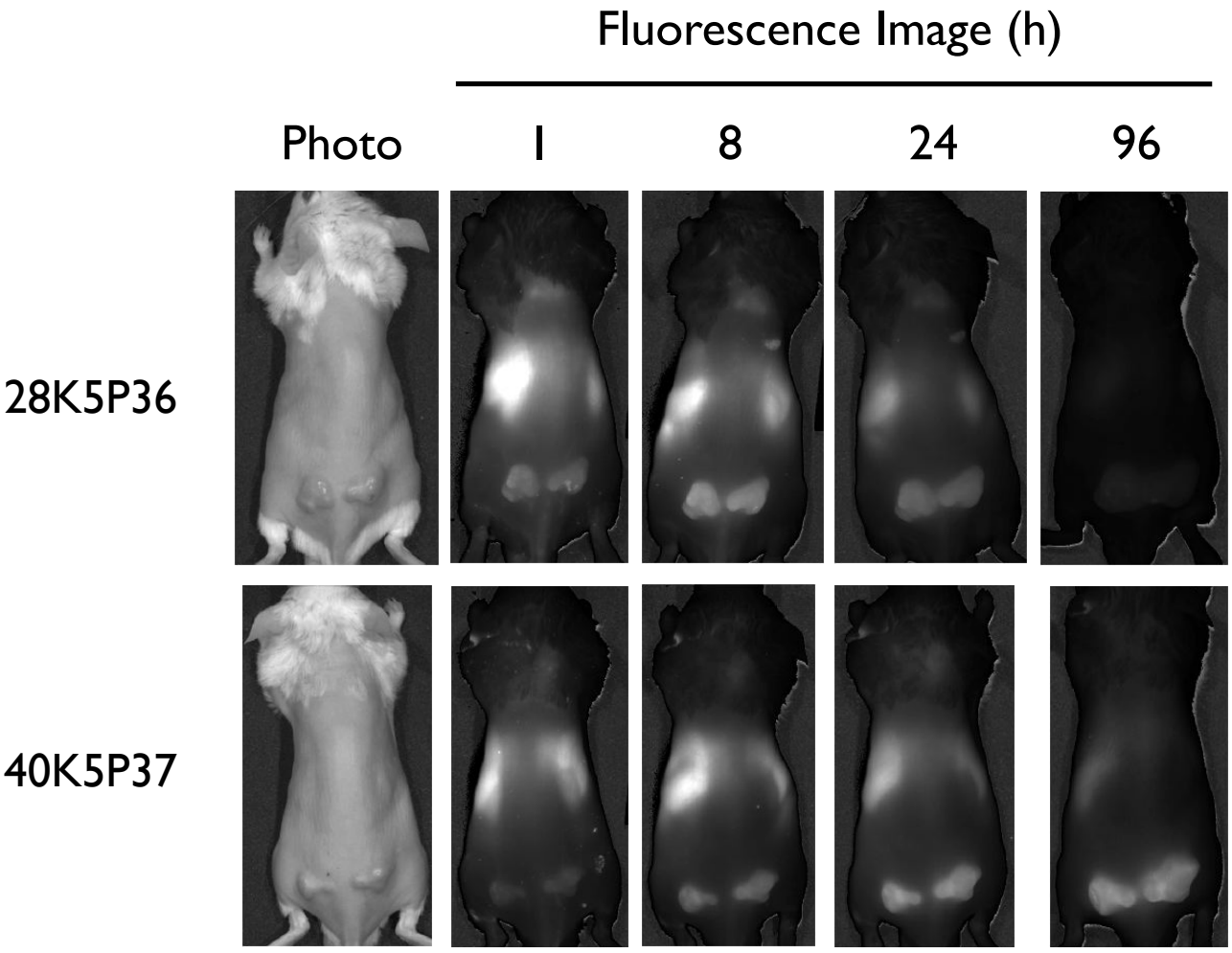

Figure 2.

B.

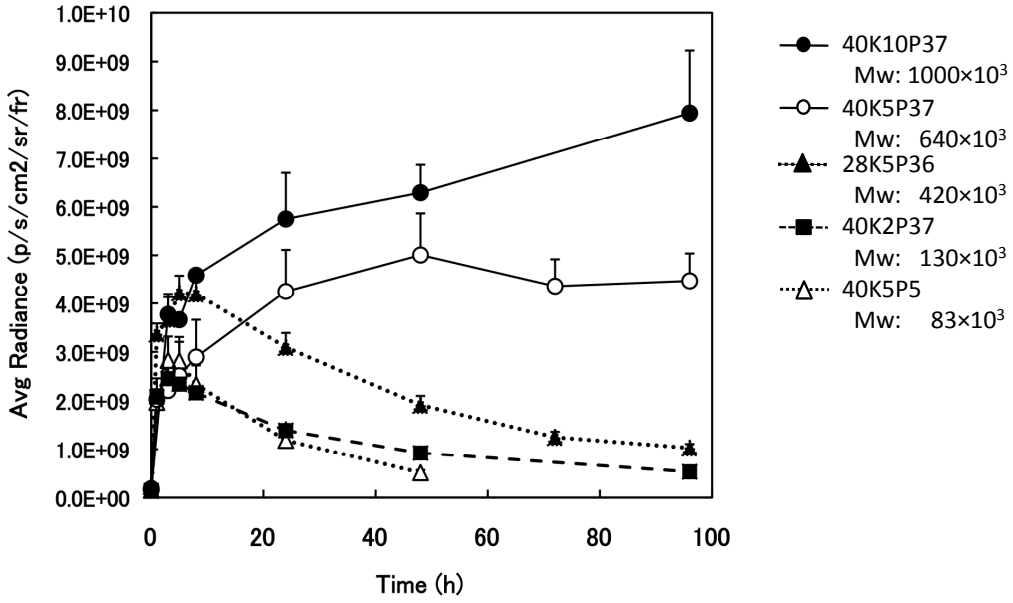
1.0E+10
9.0E+09
8.0E+09
7.0E+09
6.0E+09
5.0E+09
4.0E+09
3.0E+09
2.0E+09
1.0E+09
0.0E+00
Avg Radiance (p/s/cm2/sr/fr)
0
20
40
60
80
100
Time (h)
40K10P37
Mw: 1000×10³
40K5P37
Mw: 640×10³
28K5P36
Mw: 420×10³
40K2P37
Mw: 130×10³
40K5P5
Mw: 83×10³

Figure 3.

A

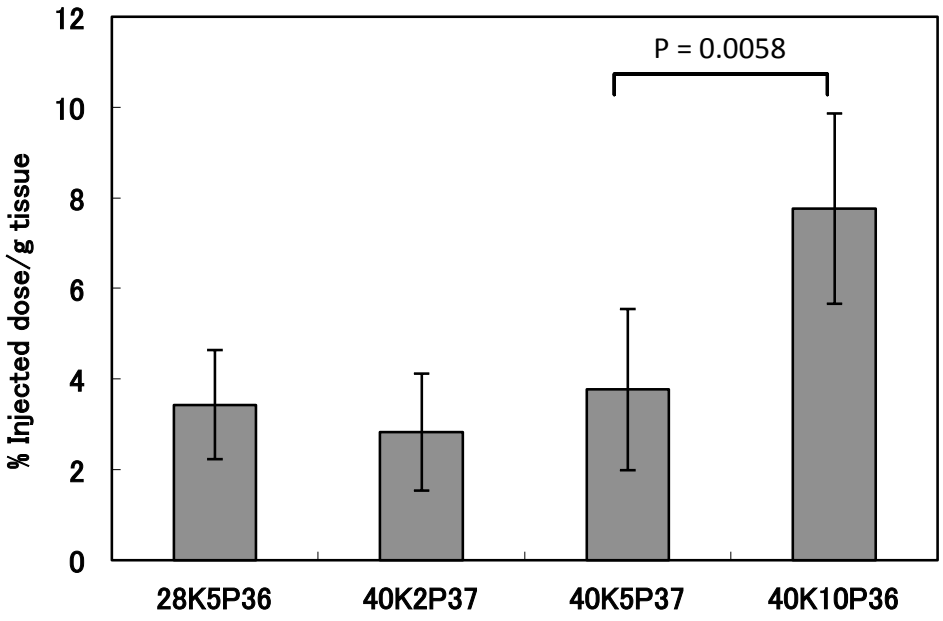
12
10
8
6
4
2
0
% Injected dose/g tissue
P = 0.0058
28K5P36
40K2P37
40K5P37
40K10P36

B

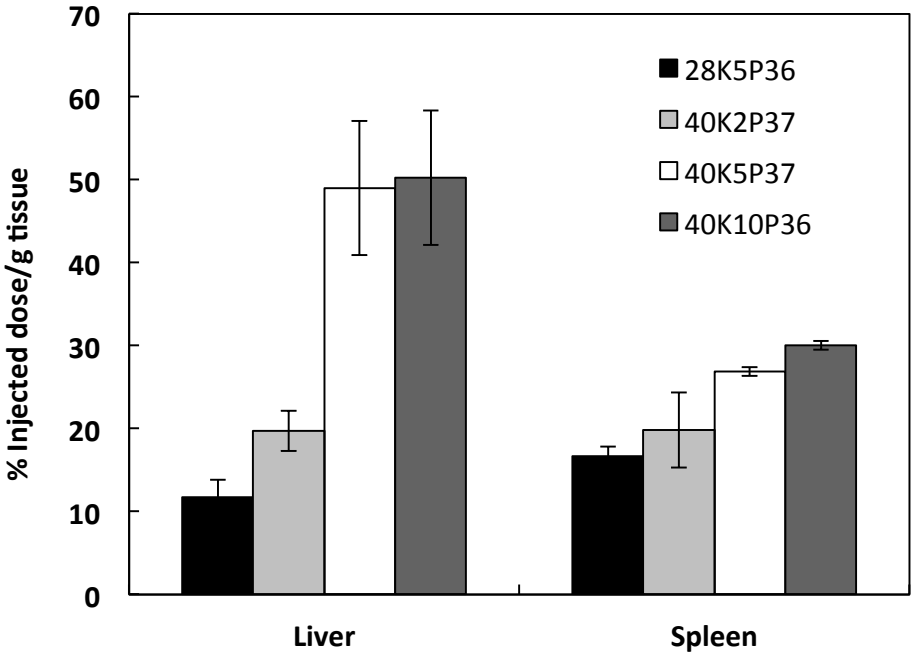
70
60
50
40
30
20
10
0
% Injected dose/g tissue
28K5P36
40K2P37
40K5P37
40K10P36
Liver
Spleen

Figure 4.

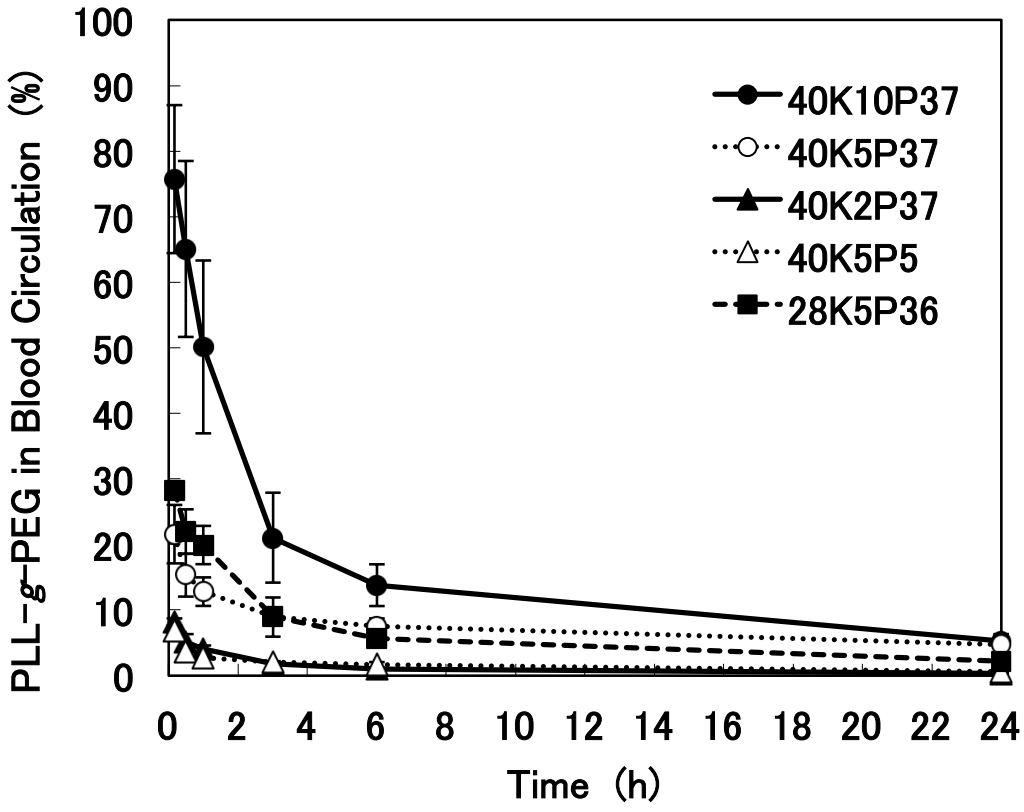
PLL-g-PEG in Blood Circulation (%)
100
90
80
70
60
50
40
30
20
10
0
0 2 4 6 8 10 12 14 16 18 20 22 24
Time (h)
40K10P37
40K5P37
40K2P37
40K5P5
28K5P36

Figure 5.

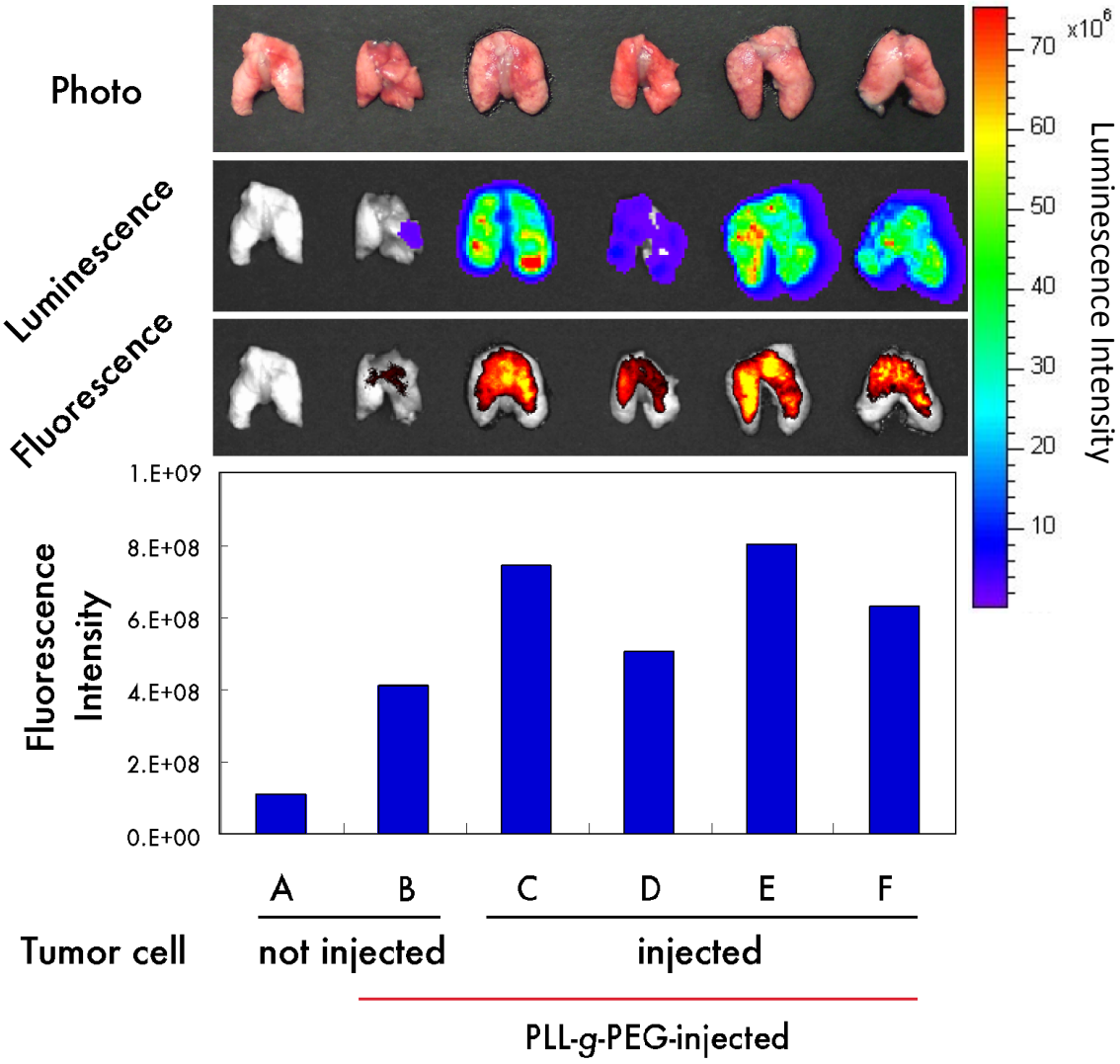
Photo
Luminescence
Fluorescence
x10^6
70
60
50
40
30
20
10
Luminescence Intensity
Fluorescence Intensity
1.E+09
8.E+08
6.E+08
4.E+08
2.E+08
0.E+00
A
B
C
D
E
F
Tumor cell
not injected
injected
PLL-g-PEG-injected

Figure 6.

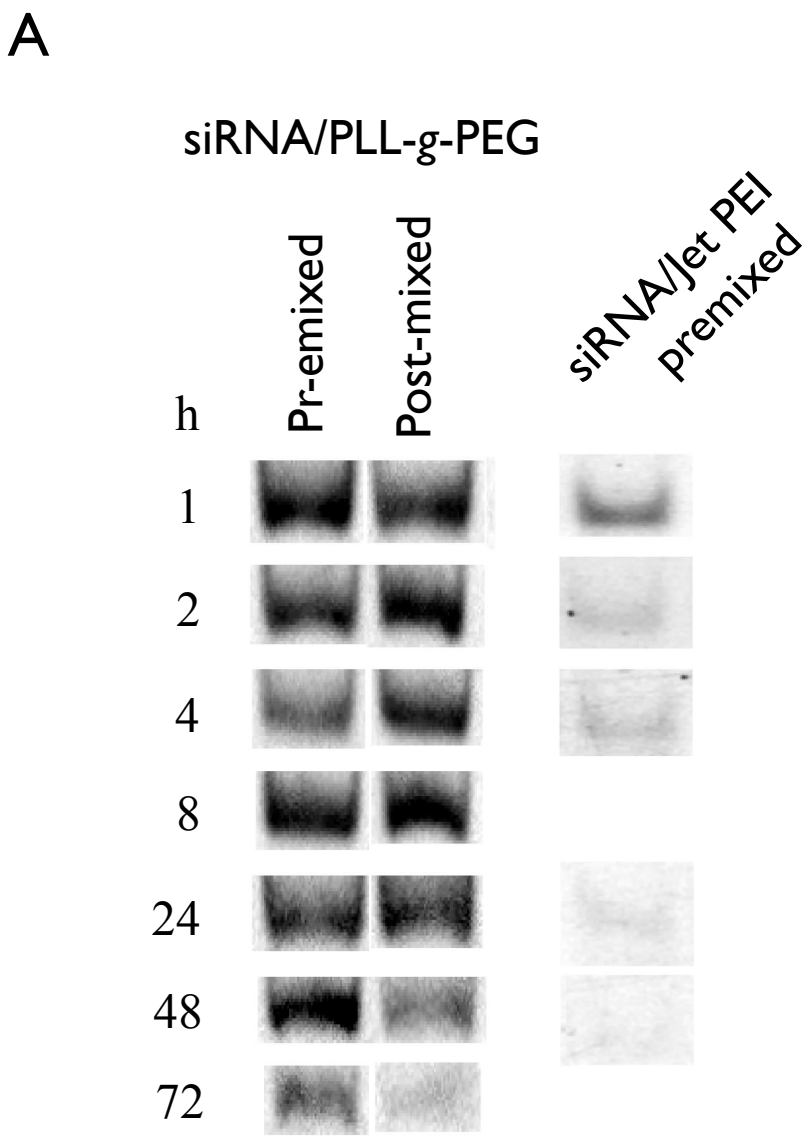
A
siRNA/PLL-g-PEG
Pr-emixed
Post-mixed
siRNA/Jet PEI
premixed
h
1
2
4
8
24
48
72

Figure 6.

B

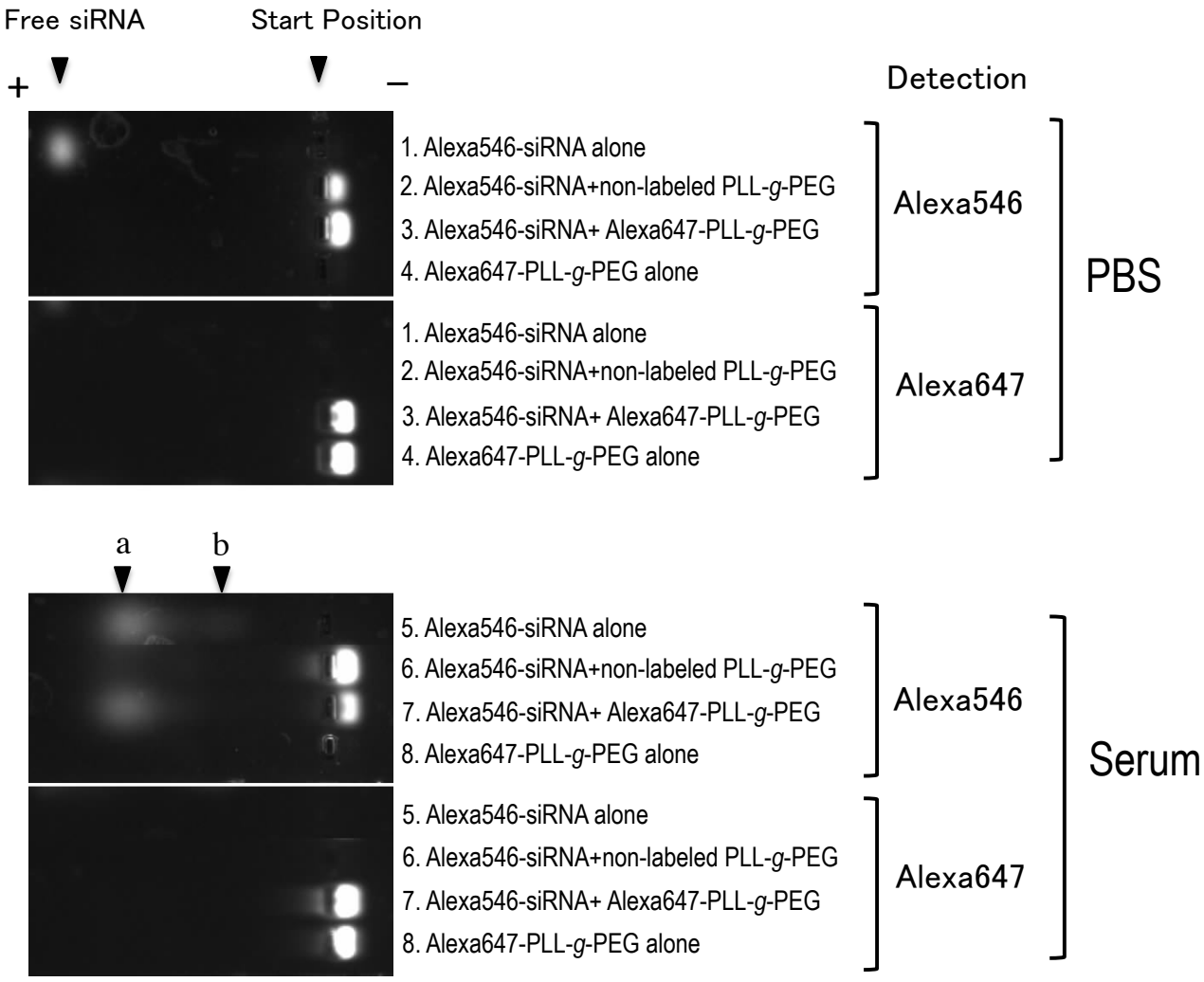
Free siRNA
Start Position
+
–
Detection
1. Alexa546-siRNA alone
2. Alexa546-siRNA+non-labeled PLL-g-PEG
3. Alexa546-siRNA+ Alexa647-PLL-g-PEG
4. Alexa647-PLL-g-PEG alone
Alexa546
1. Alexa546-siRNA alone
2. Alexa546-siRNA+non-labeled PLL-g-PEG
3. Alexa546-siRNA+ Alexa647-PLL-g-PEG
4. Alexa647-PLL-g-PEG alone
Alexa647
PBS
a
b
5. Alexa546-siRNA alone
6. Alexa546-siRNA+non-labeled PLL-g-PEG
7. Alexa546-siRNA+ Alexa647-PLL-g-PEG
8. Alexa647-PLL-g-PEG alone
Alexa546
5. Alexa546-siRNA alone
6. Alexa546-siRNA+non-labeled PLL-g-PEG
7. Alexa546-siRNA+ Alexa647-PLL-g-PEG
8. Alexa647-PLL-g-PEG alone
Alexa647
Serum